Change in Drusen Area Over Time Compared Using Spectral-Domain Optical Coherence Tomography and Color Fundus Imaging

Giovanni Gregori,[1] Zohar Yehoshua,[1] Carlos Alexandre de Amorim Garcia Filho,[1] SriniVas R. Sadda,[2] Renata Portella Nunes,[1] William J. Feuer,[1] and Philip J. Rosenfeld[1]

[1]Bascom Palmer Eye Institute, University of Miami Miller School of Medicine, Miami, Florida, United States
[2]Doheny Eye Institute, David Geffen School of Medicine, University of California-Los Angeles, Los Angeles, California, United States

Correspondence: Giovanni Gregori, Bascom Palmer Eye Institute, 1683 NW 10th Avenue, Miami, FL 33136, USA; ggregori@med.miami.edu.

Submitted: July 18, 2014
Accepted: October 6, 2014

Citation: Gregori G, Yehoshua Z, Garcia Filho CAA, et al. Change in drusen area over time compared using spectral-domain optical coherence tomography and color fundus imaging. *Invest Ophthalmol Vis Sci*. 2014;55:7662–7668. DOI:10.1167/iovs.14-15273

Purpose. To investigate the relationship between drusen areas measured with color fundus images (CFIs) and those with spectral-domain optical coherence tomography (SDOCT).

Methods. Forty-two eyes from thirty patients with drusen in the absence of geographic atrophy were recruited to a prospective study. Digital color fundus images and SDOCT images were obtained at baseline and at follow-up visits at 3 and 6 months. Registered, matched circles centered on the fovea with diameters of 3 mm and 5 mm were identified on both CFIs and SDOCT images. Spectral-domain OCT drusen measurements were obtained using a commercially available proprietary algorithm. Drusen boundaries on CFIs were traced manually at the Doheny Eye Institute Image Reading Center.

Results. Mean square root drusen area (SQDA) measurements for the 3-mm circles on the SDOCT images were 1.451 mm at baseline and 1.464 mm at week 26, whereas the measurements on CFIs were 1.555 mm at baseline and 1.584 mm at week 26. Mean SQDA measurements from CFIs were larger than those from the SDOCT measurements at all time points ($P = 0.004$ at baseline, $P = 0.003$ at 26 weeks). Changes in SQDA over 26 weeks measured with SDOCT were not different from those measured with CFIs (mean difference = 0.014 mm, $P = 0.5$).

Conclusions. Spectral-domain OCT drusen area measurements were smaller than the measurements obtained from CFIs. However, there were no differences in the change in drusen area over time between the two imaging modalities. Spectral-domain OCT measurements were considerably more sensitive in assessing drusen area changes.

Keywords: age-related macular degeneration, color fundus photography, drusen, optical coherence tomography

Drusen are one of the earliest clinical signs of age-related macular degeneration (AMD) and are well known to be important risk factors for progression to late AMD.[1–6] In particular, large soft drusen are associated with a higher risk for disease progression.[1,7–9] Color fundus images (CFIs) have long represented the gold standard for defining and evaluating drusen and the clinical stages of AMD.[10] Parameters such as total drusen area and maximum drusen size can be calculated from CFIs and have been used to predict the likelihood of progression to late AMD.[11,12]

Although the drusen burden in the macula has proven to be clinically important, it is difficult in practice to assess the drusen burden from CFIs in an accurate and reproducibly quantitative manner. Factors such as variability of fundus pigmentation, drusen appearance, and medium opacities result in large variations in assessing independent area measurements by different experts.[13,14] A number of automated and semi-automated algorithms for drusen segmentation from CFIs have been proposed,[15] but because of the difficulties mentioned above, their clinical use has been limited. Even in important clinical studies such as the Age-Related Eye Disease Study (AREDS), measurements of drusen area have been limited to a coarse grading scale obtained by visual inspection.[16]

Spectral-domain optical coherence tomography (SDOCT) has provided clinicians with high-resolution images offering an accurate representation of the geometry of the macula in three dimensions. In particular, SDOCT datasets have been used to describe the deformations of the retinal pigment epithelium (RPE) typically associated with drusen.[17–21] Fully automated algorithms for the computation of parameters such as drusen area and volume have recently been introduced.[19,22–24] Some of these algorithms have been shown to be quite robust and reproducible.[19,22,25] The ability to quickly and easily obtain precise measurement of the drusen burden can potentially be quite significant for the clinical understanding of AMD, making it possible for the clinician to monitor small changes in drusen geometry over time, and has lead to a better understanding of the dynamic nature of drusen.[26]

Relationships between drusen as defined as yellowish pigmentary changes on color fundus photography and drusen as defined as RPE deformations have been investigated.[27–30] Good overall correlation between measurements of drusen area using SDOCT and CFIs have been reported, but there are

important differences between what is captured by the two technologies. Differences in the pointwise agreement between the segmented drusen areas on SDOCT and CFIs are due to the intrinsic differences in how drusen are defined by the two imaging strategies. Spectral-domain OCT imaging identifies drusen by the presence of RPE deformations, which may not always exactly correspond to the yellowish pigmented changes seen on CFIs. Conversely, pigmentary changes may or may not represent elevations of the RPE. Moreover, different segmentation algorithms may have different characteristics. Typically, there may be some trade-off between speed and accuracy, so that the fast, robust algorithms suitable for use with commercial instruments may have a reduced sensitivity to detect small drusen and drusen with little if any elevation of the RPE.[19,23,28]

We compared drusen measurements from manually segmented CFIs with drusen measurements obtained using SDOCT fully automated algorithm developed at the Bascom Palmer Eye Institute. This algorithm, a version of which is now commercially available with the Cirrus HD-OCT instrument (software version 6.0; Carl Zeiss Meditec, Dublin, CA, USA), provides a quantitative assessment of RPE deformations and generates measurements of drusen volume and area. These drusen area measurements from SDOCT images were shown to be highly reproducible,[19,25] although typically smaller than those on color fundus images.[28,29] The pointwise agreement between the segmented drusen areas using the two different modalities was only fair, as the OCT algorithm tends to overlook small, flat drusen and subretinal drusenoid deposits. Despite these limitations, it is clear that the SDOCT algorithm produces meaningful measurements of the drusen burden in a given eye. These measurements are particularly representative for the medium and larger sized drusen, which may be the most clinically meaningful features for disease progression. Therefore, if drusen burden can be used as a surrogate marker to predict disease progression, then it is important to understand how SDOCT and CFI measurements of drusen area compare over time.

The purpose of this prospective study was to compare the measurements of drusen area from manual outlines on CFIs with those generated by our automated algorithm on SDOCT datasets. Changes in drusen area obtained using the two different modalities were compared over 6 months.

Methods

This prospective study was approved by the institutional review board of the University of Miami Miller School of Medicine and was compliant with the Health Insurance Portability and Accountability Act of 1996. A total of 30 patients from the retina service were enrolled at the Bascom Palmer Eye Institute between November 1, 2009, and May 3, 2011. Each patient signed an informed consent. The Bascom Palmer Eye Institute retina faculty confirmed the clinical diagnosis of nonexudative AMD. Eligibility criteria included an age of 50 years or more, the presence of high-risk drusen in the study eye, and best-corrected visual acuity of 20/63 or better (an Early Treatment Diabetic Retinopathy Study [ETDRS] letter score of at least 59). High-risk drusen were defined by the presence of at least one druse with a diameter of at least 250 μm observed on fundus biomicroscopy or color fundus photography and a total drusen volume of at least 0.03 mm^3 as measured by SDOCT within a 3-mm-diameter circle centered on the fovea. Digital photography, fluorescein angiography, and OCT images were obtained to document the absence of choroidal neovascularization prior to including patients in the study. Eyes with geographic atrophy were excluded from this study. Patients with other concomitant retinal pathologies, including pathologic myopia, diabetic retinopathy, hypertensive retinopathy, and central serous chorioretinopathy, were excluded.

Digital color fundus images and SDOCT images (Cirrus HD-OCT), were obtained at baseline and at follow-up visits at 3 and 6 months. Spectral-domain OCT macular cube scans (200 × 200 A-scans) were obtained after pupil dilation, using one drop of 2.5% phenylephrine hydrochloride and 1% tropicamide. Each scan covered a retinal area of 6 × 6 mm centered on the fovea. A single experienced operator, who assessed the quality of the scan during its acquisition, performed all scans. Whenever possible, an effort was made to delete datasets with poor signal strength or with significant motion artifacts.

After acquisition, one of the authors reviewed each scan. At least one good quality scan (strength equal to or greater than 7 and no clear evidence of motion artifacts) was confirmed for each eye in the study at each time point. If more than one good quality scan was available for a given eye at a time point, then one scan was randomly chosen.

Raw OCT datasets were exported to a personal computer and analyzed as previously described.[19] The position of the fovea was determined manually by scanning through the OCT dataset and finding the spot where the geometry of the inner retinal layers best matched the known anatomical configuration in the fovea. A proprietary algorithm was used to find the RPE and the RPE floor. The RPE floor is an extrapolated virtual RPE surface representing the geometry of an RPE free of local deformations associated with drusen, and the difference between the actual RPE segmentation and the RPE floor defines the drusen thickness map.[19] Drusen area and volume measurements were then obtained for the macular areas within circles centered on the fovea, with diameters of 3 mm (C3) and 5 mm (C5) as well as for the full dataset.[19]

Each SDOCT dataset was registered to the corresponding color fundus image by using the OCT fundus image (OFI) and the en face retinal vascular patterns. Ad hoc software was developed to register CFIs to the OFIs.[31] This software also identified regions on CFIs matching the 3- and 5-mm circles centered on the fovea on the SDOCT datasets (Fig. 1). Results of the automatic registration were reviewed by one of the authors, and manual adjustments were made if the original registration was deemed unsatisfactory. Drusen within the 3- and 5-mm circles on CFIs were then manually outlined and measured (Fig. 2) by experienced graders at the Doheny Eye Institute Image Reading Center.[28]

As discussed in previous reports,[19,28] a square root transformation of the drusen area data was performed prior to statistical manipulation of the measurements. This transformation eliminated the dependence of the measurement variance on lesion size and permitted a more accurate assessment of whether the lesion area had changed. All data are therefore presented here using the square root of the drusen area measurements (SQDA). Measurements of drusen area from SDOCT datasets and CFIs were compared using the paired *t*-test. Agreement between SDOCT and color fundus area measurements is summarized by the intraclass correlation coefficient. All analyses were performed with SPSS version 19 software (SPSS, Inc., Chicago, IL, USA).

Results

Forty-two eyes from the 30 patients enrolled satisfied inclusion criteria at baseline. Measurements from the C3 and C5 regions from both SDOCT images and CFIs were obtained for all eyes at baseline, at 12 weeks, and at 26 weeks. Two patients (four eyes) withdrew from the study before 26 weeks. One eye

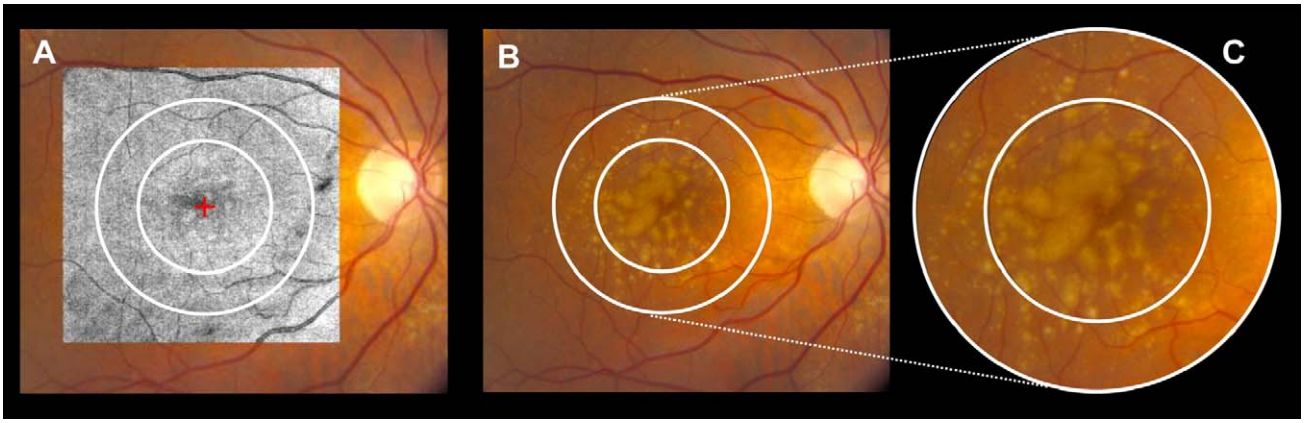

FIGURE 1. Registration of color and OCT fundus images. (**A**) *Circles* with diameters of 3 mm and 5 mm are centered on the fovea and marked on the spectral-domain optical coherence tomography fundus image (OFI), which is registered with the color fundus image (CFI). (**B**) *Circles* with diameters of 3-mm and 5-mm circles are transferred from the OFI to the CFI. (**C**) The CFI area contained within the circles was isolated and sent to the Doheny Image Reading Center for manual grading.

progressed to neovascular disease during the study, and another eye could not be graded by the reading center due to poor quality of the CFIs. Drusen area measurements for 36 eyes from 27 patients were analyzed.

Generally, the measurements for drusen area from CFIs were larger than those from SDOCT at all time points (Fig. 3 [figures show data only in C3]). Mean SQDA in the 3-mm circles for the SDOCT scans were 1.451 mm at baseline and 1.464 mm at 26 weeks. Mean SQDA in the 3-mm circles for CFIs were 1.555 mm at baseline and 1.584 mm at 26 weeks. Mean SQDA in the 5-mm circles for the SDOCT scans were 1.673 mm at baseline and 1.710 mm at 26 weeks. Mean SQDA in the 5-mm circles for CFIs were 1.950 mm at baseline and 1.996 mm at 26 weeks. Differences between the area measurements on the CFIs and those from SDOCT scans were statistically significant at baseline and at 26 weeks, both in C3 and C5 (all $P < 0.004$). The intraclass correlation coefficient of agreement between the modalities for the 3-mm measurements was 0.79 at baseline and 0.81 at 26 weeks. In the C5 region, the intraclass correlation coefficient was 0.70 at baseline and 0.71 at 26 weeks.

The change in SQDA over 26 weeks clearly identifies two different populations when measured with SDOCT (Fig. 4A). Two eyes had a statistically significant loss in drusen area (i.e., change outside the 95% test–retest tolerance limits for SDOCT measurements[26]). Moreover, in these two eyes, the loss in drusen area was immediately apparent and considerably beyond threshold for statistical significance, whereas the change in SQDA for all other eyes was normally distributed (Fig. 5B), with a statistically significant mean SQDA growth of 0.064 mm in C3 ($P < 0.001$). The two eyes with drusen area loss on SDOCT also showed the largest loss in drusen area on CFIs, but only one of these eyes could clearly be identified as an outlier from CFI measurements (Fig. 4B). The change in SQDA for all other eyes showed a statistically significant mean growth of 0.073 mm when measured on CFIs in C3 ($P = 0.002$). The change in SDQA over 26 weeks in C5 showed the same behavior as that described in C3, with significant mean SQDA growth of 0.086 mm ($P < 0.001$) on SDOCT and 0.089 mm ($P = 0.003$) on CFIs, when removing the two eyes with clear loss of drusen area.

Differences between the changes in SQDA over 26 weeks measured with SDOCT and those measured with CFI (Fig. 5A) were not significantly different from 0, with a mean of 0.015 mm ($P = 0.5$) in C3 and a mean of 0.010 mm in C5 ($P = 0.7$). The median of the differences in SQDA changes was also not significantly different from 0, with values equal to 0.004 mm ($P = 0.51$, Wilcoxon) in C3 and 0.02 mm ($P = 0.62$, Wilcoxon test) in C5. The statistical distributions of changes in SQDA were similar for both modalities, showing an essentially normal looking distribution with positive mean and large negative outliers (Fig. 5B). The spread of the changes in SQDA was larger when measured on CFIs than on SDOCT: The

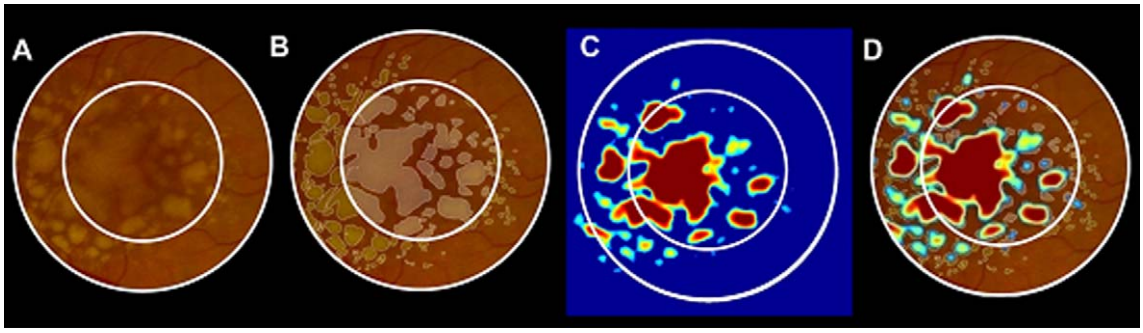

FIGURE 2. Drusen areas were measured with different imaging modalities. (**A**) Central 3-mm and 5-mm *circles* were superimposed on a color fundus image (CFI). (**B**) Manually outlined drusen on the CFI, as shown in (**A**). (**C**) Automated drusen area map was calculated using the spectral-domain optical coherence tomography (SDOCT) algorithm. (**D**) Composite image shows the manually outlined drusen shown in (**B**) and the automated drusen map shown in (**C**).

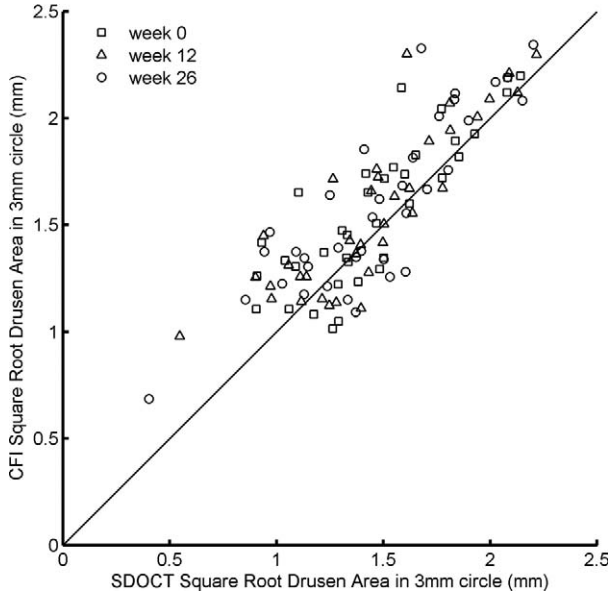

FIGURE 3. Comparison of the square root drusen area measurements within the central 3-mm circle obtained using color fundus images (CFI) and spectral-domain optical coherence tomography (SDOCT). *Solid line* is the bisector.

interquartile range was 0.11 mm greater on CFIs in C3 and 0.14 mm greater on CFIs in C5.

DISCUSSION

Over the past few years, a number of studies have shown that quantitative descriptions of the RPE geometry can be obtained from SDOCT datasets. As new SDOCT algorithms characterizing drusen load in the central macula are introduced and become widely available with commercial OCT instruments, it is important to understand the relationship between these parameters and the standard measurements of drusen from CFIs. To better understand this relationship, we compared measurements of drusen area using CFIs and SDOCT datasets over time.

Area measurements of drusen, identified by experienced graders on CFIs within a 3- and 5-mm circle centered at the fovea, were found to be typically greater than the area measurements obtained using SDOCT imaging and an automated detection algorithm. These results are consistent with our previous study.[28] Indeed, we found here a somewhat better agreement between CFIs and SDOCT than that in results published by Yehoshua et al.[28] For instance, in C3, we obtained an intraclass correlation coefficient of agreement of 0.79 vs. 0.60 with ICC, as reported by Yehoshua et al.[28] The higher correlation might be due to the fact that our eligibility criteria resulted in a population with a somewhat heavier drusen load. As we previously discussed,[19,28] differences between the measurements of these two modalities can be explained by the fact that drusen are defined on CFIs based on macular pigment abnormalities, whereas drusen are defined on SDOCT images by their deformation of RPE geometry. There are several possible situations resulting in disagreements between the measurements on CFIs and the measurements on OCT datasets, the most common being the identification of drusen on fundus images that did not significantly elevate the RPE. These include drusen that correspond to small RPE deformations seen in the OCT images and might possibly be detected by a more sensitive algorithm, as well as drusen for which the OCT images show no appreciable RPE deformation. Recently, Diniz et al.[29] analyzed a group of 40 eyes by using essentially the same SDOCT algorithm. They reported that SDOCT measurements found a smaller number of drusen, in total as well as in all size groups (small, intermediate, and large), than manual segmentation of CFIs. However, in their population, the mean drusen area from SDOCT was actually larger, although not significantly so, than the CFIs mean drusen area. The outcome about mean drusen area in the publication by

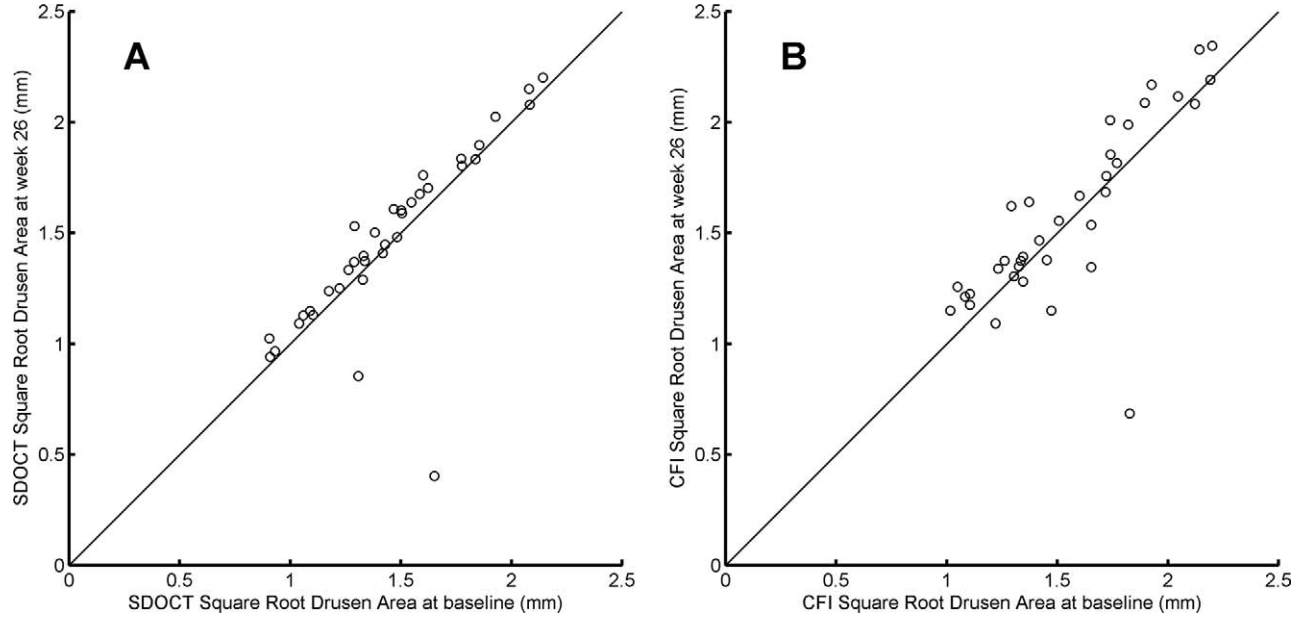

FIGURE 4. Changes in square root drusen area (SQDA) measurements within the central 3-mm circle. (**A**) Square root drusen area at baseline versus SQDA at week 26, obtained using spectral-domain optical coherence tomography (SDOCT). (**B**) Square root drusen area at baseline versus SQDA at 26 weeks, obtained using color fundus images (CFI). *Solid line* is the bisector.

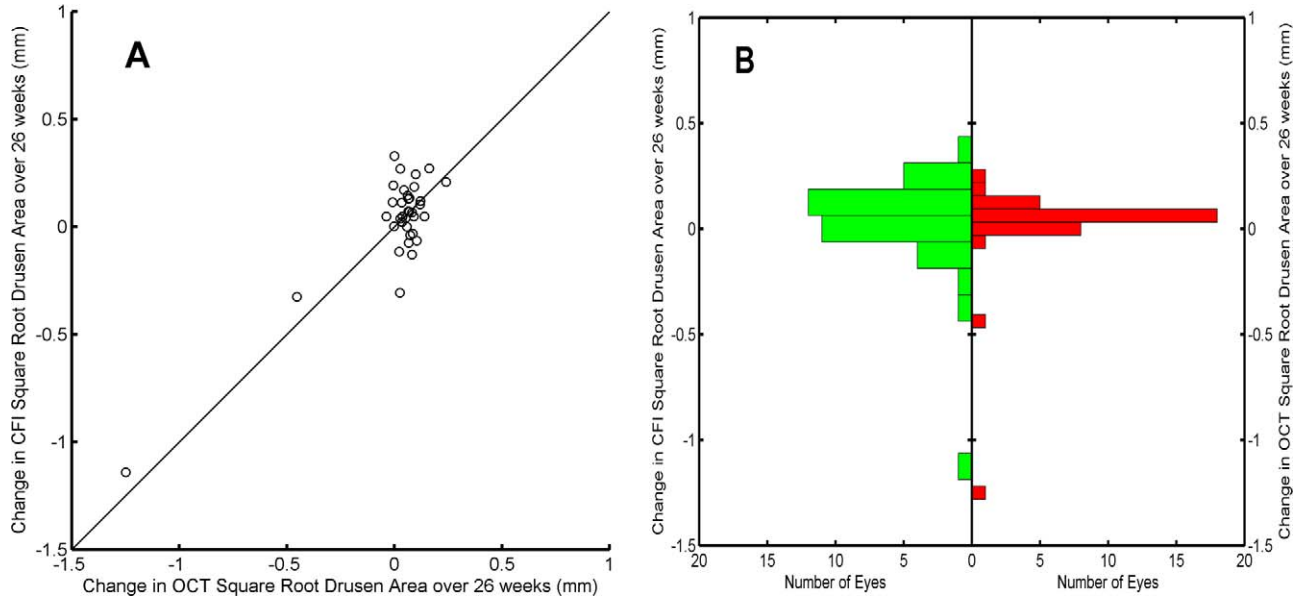

FIGURE 5. Changes in square root drusen area (SQDA) measurements within the central 3-mm circle over 26 weeks. (**A**) Change in SQDA was obtained using spectral-domain optical coherence tomography (SDOCT) images versus changes in SQDA obtained using color fundus images (CFIs). *Solid line* is the bisector. (**B**) Histograms of the changes in SQDA as measured with CFIs (*left*) and SDOCT (*right*).

Diniz et al.[29] is different from ours in the present study (as well as that previously published by our group[28]) and somewhat surprising, particularly in view of their results of drusen distribution by imaging modality (Fig. 5A in their paper). It is clear that in some eyes, the drusen area on SDOCT can be larger than on CFIs (e.g., see the study by Yehoshua et al.[28]). Although this situation is relatively infrequent in our population (Fig. 3), it should be assumed that such eyes play a larger role in the sample of eyes analyzed by Diniz et al.[29]

We have previously shown that SDOCT drusen measurements are very reproducible and can be used to study drusen dynamics, which can serve as a surrogate for disease progression over a relatively short period of time.[19,25] The data presented here also confirm results from our natural history study of drusen.[26] Mean drusen area and volume tend to grow slowly over time, whereas in some eyes, we found a significant and sudden loss in drusen area. Our results, particularly the distribution of SQDA changes shown in Figures 4 and 5, clearly show that SDOCT measurements are much more precise than those from CFIs and are more sensitive to underlying changes in drusen morphology. In particular, there were two eyes in which SDOCT measurements had a pronounced loss in drusen area over 26 weeks, but the measurements from fundus images only clearly identified significant change in one eye.

Although we know that SDOCT measurements of drusen are somewhat different than the ones obtained from CFIs, our data show that there are no significant differences between the mean changes in drusen area over time, measured with each of the two modalities. It is important to stress that, although SDOCT area measurements are systematically smaller than the ones obtained from CFIs, this bias disappears when we consider the changes in drusen area over time. Moreover, the shape of the statistical distribution of the changes in SQDA with CFI appears to be substantially similar to the one obtained with SDOCT (Fig. 5). This suggests that both modalities capture essentially the same changes in drusen area over time. Our result can be explained by noticing that most of the changes in drusen area are caused by changes in the morphology of large soft drusen, particularly in the central macular region, whereas the most common differences between the measurements with SDOCT and those with CFIs at any given time point are caused by small hard drusen.

One potential weakness of our study is the relatively short length of follow-up. It certainly would be interesting to study patients over longer time intervals and, ideally, analyze data prior to conversion to advanced AMD. However, 6 months is enough to establish a definite change in drusen area measurements and establish a significant comparison between the two modalities.

Manual segmentation of drusen from SDOCT datasets is in good agreement with CFI drusen measurements, although there are some clear differences between the anatomical features assessed by the two modalities.[27] However, manual segmentation of drusen is costly and time consuming. In contrast, a fully automated algorithm, such as the one studied here, whereas it might underestimate small, flat drusen, provides a fast, inexpensive, and reproducible approach for identifying and following drusen. These measurements are particularly representative for the medium and larger sized drusen, which should be more clinically meaningful when assessing disease severity and progression. Furthermore, the excellent reproducibility[19] of our SDOCT measurements results in much higher sensitivity to detection of differences in SQDA and a much tighter distribution of the changes in SQDA over time (Fig. 5B).

It should be mentioned that a number of recent works have also considered drusen measurement from OCT images acquired using polarization sensitive instruments. In this setting, new segmentation algorithms have been proposed, taking advantage of the depolarizing properties of the RPE as a way to identify this layer.[32,33]

Our results provide further evidence for the relevance of automated SDOCT drusen measurements in evaluating drusen dynamics. Such algorithms may be useful in developing improved severity scales to predict disease progression and in clinical trials as novel endpoints when assessing potential therapies to slow the progression to nonexudative AMD.[34] In addition, the widespread availability of this particular algorithm

with the Cirrus HD-OCT instrument (software version 6.0 and later) provides the clinician with a rapid, reproducible, quantitative approach for following normal disease progression in patients with nonexudative AMD.

Acknowledgments

Disclosure: **G. Gregori**, Carl Zeiss Meditec, Inc. (F), P; **Z. Yehoshua**, None; **C.A.A. Garcia Filho**, Carl Zeiss Meditec, Inc. (F); **S.R. Sadda**, Carl Zeiss Meditec, Inc. (F), Genentech (C, F), Optos (C, F), Allergan (C, F), Roche (C), Alcon (C); **R. Portella Nunes**, Carl Zeiss Meditec, Inc. (F); **W.J. Feuer**, None; **P.J. Rosenfeld**, Carl Zeiss Meditec, Inc. (F), Acucela (C, F), Advanced Cell Technology (F), GlaxoSmithKline (F), Alcon (C), Bayer (C), Boehringer Ingelheim (C), Chengdu Kanghong Biotech (C), Healios KK (C), Merck (C), Oraya (C), Roche (C), Sanofi/Genzyme (C), Xcovery Vision (C)

References

1. Ferris FL, Davis MD, Clemons TE, et al. A simplified severity scale for age-related macular degeneration: AREDS Report No. 18. *Arch Ophthalmol*. 2005;123:1570–1574.
2. Klein R, Klein BE, Tomany SC, Meuer SM, Huang GH. Ten-year incidence and progression of age-related maculopathy: The Beaver Dam eye study. *Ophthalmology*. 2002;109:1767–1779.
3. Bressler SB, Maguire MG, Bressler NM, Fine SL. Relationship of drusen and abnormalities of the retinal pigment epithelium to the prognosis of neovascular macular degeneration. The Macular Photocoagulation Study group. *Arch Ophthalmol*. 1990;108:1442–1447.
4. van Leeuwen R, Klaver CC, Vingerling JR, Hofman A, de Jong PT. The risk and natural course of age-related maculopathy: follow-up at 6 1/2 years in the Rotterdam study. *Arch Ophthalmol*. 2003;121:519–526.
5. Wang JJ, Foran S, Smith W, Mitchell P. Risk of age-related macular degeneration in eyes with macular drusen or hyperpigmentation: the Blue Mountains Eye Study cohort. *Arch Ophthalmol*. 2003;121:658–663.
6. Seddon JM, Sharma S, Adelman RA. Evaluation of the clinical age-related maculopathy staging system. *Ophthalmology*. 2006;113:260–266.
7. Pauleikhoff D, Barondes MJ, Minassian D, Chisholm IH, Bird AC. Drusen as risk factors in age-related macular disease. *Am J Ophthalmol*. 1990;109:38–43.
8. Klein R, Klein BE, Knudtson MD, Meuer SM, Swift M, Gangnon RE. Fifteen-year cumulative incidence of age-related macular degeneration: the Beaver Dam eye study. *Ophthalmology*. 2007;114:253–262.
9. Ferris FL III, Wilkinson CP, Bird A, et al. Clinical classification of age-related macular degeneration. *Ophthalmology*. 2013; 120:844–851.
10. Bartlett H, Eperjesi F. Use of fundus imaging in quantification of age-related macular change. *Surv Ophthalmol*. 2007;52: 655–671.
11. The Age-Related Eye Disease Study Research Group. The age-related eye disease study system for classifying age-related macular degeneration from stereoscopic color fundus photographs: the age-related eye disease study report number 6. *Am J Ophthalmol*. 2001;132:668–681.
12. Bird AC, Bressler NM, Bressler SB, et al. An international classification and grading system for age-related maculopathy and age-related macular degeneration. The International ARM Epidemiological Study Group. *Surv Ophthalmol*. 1995;39: 367–374.
13. Pirbhai A, Sheidow T, Hooper P. Prospective evaluation of digital non-stereo color fundus photography as a screening tool in age-related macular degeneration. *Am J Ophthalmol*. 2005;139:455–461.
14. Scholl HP, Peto T, Dandekar S, et al. Inter- and intra-observer variability in grading lesions of age-related maculopathy and macular degeneration. *Graefes Arch Clin Exp Ophthalmol*. 2003;241:39–47.
15. Kanagasingam Y, Bhuiyan A, Abramoff MD, Smith RT, Goldschmidt L, Wong TY. Progress on retinal image analysis for age related macular degeneration. *Prog Retin Eye Res*. 2014;38: 20–42.
16. Davis MD, Gangnon RE, Lee LY, et al. The Age-Related Eye Disease Study severity scale for age-related macular degeneration: AREDS report no. 17. *Arch Ophthalmol*. 2005;123: 1484–1498.
17. Yi K, Mujat M, Park BH, et al. Spectral domain optical coherence tomography for quantitative evaluation of drusen and associated structural changes in non-neovascular age-related macular degeneration. *Br J Ophthalmol*. 2009;93:176–181.
18. Freeman SR, Kozak I, Cheng L, et al. Optical coherence tomography-raster scanning and manual segmentation in determining drusen volume in age-related macular degeneration. *Retina*. 2009;30:431–435.
19. Gregori G, Wang F, Rosenfeld PJ, et al. Spectral domain optical coherence tomography imaging of drusen in nonexudative age-related macular degeneration. *Ophthalmology*. 2011;118: 1373–1379.
20. Leuschen JN, Schuman SG, Winter KP, et al. Spectral-domain optical coherence tomography characteristics of intermediate age-related macular degeneration. *Ophthalmology*. 2013;120: 140–150.
21. Farsiu S, Chiu SJ, O'Connell RV, et al. Quantitative classification of eyes with and without intermediate age-related macular degeneration using optical coherence tomography. *Ophthalmology*. 2014;121:162–172.
22. Chiu SJ, Izatt JA, O'Connell RV, Winter KP, Toth CA, Farsiu S. Validated automatic segmentation of AMD pathology including drusen and geographic atrophy in SD-OCT images. *Invest Ophthalmol Vis Sci*. 2012;53:53–61.
23. Iwama D, Hangai M, Ooto S, et al. Automated assessment of drusen using three-dimensional spectral-domain optical coherence tomography. *Invest Ophthalmol Vis Sci*. 2012;53: 1576–1583.
24. Chen Q, Leng T, Zheng L, et al. Automated drusen segmentation and quantification in SD-OCT images. *Med Image Anal*. 2013;17:1058–1072.
25. Nittala MG, Ruiz-Garcia H, Sadda SR. Accuracy and reproducibility of automated drusen segmentation in eyes with non-neovascular age-related macular degeneration. *Invest Ophthalmol Vis Sci*. 2012;53:8319–8324.
26. Yehoshua Z, Wang F, Rosenfeld PJ, Penha FM, Feuer WJ, Gregori G. Natural history of drusen morphology in age-related macular degeneration using spectral domain optical coherence tomography. *Ophthalmology*. 2011;118:2434–2441.
27. Jain N, Farsiu S, Khanifar AA, et al. Quantitative comparison of drusen segmented on SD-OCT versus drusen delineated on color fundus photographs. *Invest Ophthalmol Vis Sci*. 2010; 51:4875–4883.
28. Yehoshua Z, Gregori G, Sadda SR, et al. Comparison of drusen area detected by spectral domain optical coherence tomography and color fundus imaging. *Invest Ophthalmol Vis Sci*. 2013;54:2429–2434.
29. Diniz B, Ribeiro R, Heussen FM, Maia M, Sadda S. Drusen measurements comparison by fundus photograph manual delineation versus optical coherence tomography retinal pigment epithelial segmentation automated analysis. *Retina*. 2014;34:55–62.

Investigative Ophthalmology & Visual Science

30. Schlanitz FG, Ahlers C, Sacu S, et al. Performance of drusen detection by spectral-domain optical coherence tomography. *Invest Ophthalmol Vis Sci*. 2010;51:6715–6721.
31. Li Y, Gregori G, Knighton RW, Lujan BJ, Rosenfeld PJ. Registration of OCT fundus images with color fundus photographs based on blood vessel ridges. *Opt Express*. 2011;19:7–16.
32. Baumann B, Gotzinger E, Pircher M, et al. Segmentation and quantification of retinal lesions in age-related macular degeneration using polarization-sensitive optical coherence tomography. *J Biomed Opt*. 2010;15:061704.
33. Schlanitz FG, Baumann B, Spalek T, et al. Performance of automated drusen detection by polarization-sensitive optical coherence tomography. *Invest Ophthalmol Vis Sci*. 2011;52:4571–4579.
34. Garcia Filho CA, Yehoshua Z, Gregori G, et al. Change in drusen volume as a novel clinical trial endpoint for the study of complement inhibition in age-related macular degeneration. *Ophthalmic Surg Lasers Imaging Retina*. 2014;45:18–31.

Investigative Ophthalmology & Visual Science